Electronic Supplementary Material (ESI) for ChemComm.

Design of cost-efficient and photocatalytically active Zn-based MOFs decorated with Cu_2O nanoparticles for CO_2 methanation

María Cabrero-Antonino,[a,†] Sonia Remiro-Buenamañana,[b,†] Manuel Souto,[c] Antonio A. García-Valdivia,[d] Duane Choquesillo-Lazarte,[e] Sergio Navalón,[a] Antonio Rodriguez-Diéguez,[d]* Guillermo Mínguez Espallargas,[c]* and Hemenegildo García[a,b,]*

Supporting Information

1. General methods and materials

Materials and reagents. All the reagents and solvents employed in this study were of analytical reagent or HPLC grade and were supplied by Sigma-Aldrich.

Synthesis of MOF(Zn)-1. 3H-benzotriazole-5-carboxylate (10 mg, 0.06 mmol) was dissolved in 0.5 mL of DMF before adding 0.5 mL of distilled water. Separately 16.51 mg (0.09 mmol) of $Zn(CH_3COO)_2$ was dissolved in 0.5 mL of distilled water before adding 0.5 mL of DMF. Both solutions were mixed and the resulting solution was placed in a closed glass vessel and introduced in an oven at 95 °C for 12 h, after which yellow/brown single crystals were isolated, which were washed with water/methanol. Yield: 55% based on metal. Heating at different temperatures produce different degrees of breathing as revealed by single-crystal diffraction (see below).

Synthesis of MOF(Zn)-2. MOF(Zn)-2 is obtained upon heating at 400 °C for 2 h crystals of **MOF(Zn)-1**.

Synthesis of MOF-74(Zn). Synthesis of MOF-74(Zn) was adapted from a previously reported procedure.[S1] A mixture of 2,5-hydroxy-1,4-benzenedicarboxylic acid (H_2DHBDC) (2.4 g, 12.1 mmol) and zinc nitrate tetrahydrate, $Zn(NO_3)_2{\cdot}4(H_20)$ (179 mg, 60.5 mmol) were dissolved in DMF (240 mL) and water (120 mL), dissolved and heated to 105 °C for 20 hours and then cooled to room temperature. Yellow needle crystals were obtained in yield 51 % (based on H_2DHBDC) that were washed with DMF and methanol, and dried in air.

Synthesis of MIL-125(Ti)-NH_2. MIL-125(Ti)-NH_2 was prepared following previously reported procedures.[S2] 2-Aminoterephtalic acid (1.43 g, 7.9 mmol) was dissolved in 20 mL of anhydrous N,N-dimethylformamide (DMF). Anhydrous methanol (5 mL) was then added to the reaction mixture and the system sonicated for 20 min. The reaction mixture was transferred to a Teflon-lined autoclave (50 mL) and titanium isopropoxide (1.36 g, 4.8 mmol) was subsequently added. The autoclave was sealed and heated at 110 °C for 72 h. After cooling the Teflon to room temperature, the resulting precipitate was filtered, washed with DMF at room temperature for 12 h and, then, washed with DMF at 120 °C for 12 h. This washing procedure was repeated using methanol as solvent. Finally, the solid was recovered by filtration and dried in the oven at 100 °C.

Synthesis of CuO_2@MOFs using the photodeposition method (PD). Copper NPs were deposited in the previously synthesized MOFs (MOF(Zn)-1, MOF(Zn)-2, MOF-74(Zn) and MIL-125(Ti)-NH_2) using the PD method.[S3] Each MOF was dispersed by sonication in a mixture of water (13 mL) and methanol (5 mL). Then, $Cu(NO_3)_2{\cdot}3H_2O$ was dissolved in water (2 mL) and it was added to the MOF solution at initial 1wt%. The solution was purged with argon for 20 min. Finally, the mixture was irradiated using an UV-Visible light Xe lamp (300 W) for 4 h. The resulting solid was filtered, washed with water and dried in the oven at 100 °C for 24 h.

2. Structural features of MOF(Zn)

Upon heating the as-synthetised material (**MOF(Zn)**), the solvent molecules (DMF and H_2O) are removed from the channels causing a reversible continuous shrinkage of the structure.[S4,S5] Three different MOFs with a different degree of breathing have been isolated after 2h heating at 100 °C , 200 °C, and 350 °C, denoted **MOF(Zn)-100, MOF(Zn)-200** (corresponding to **MOF(Zn)-1**), and **MOF(Zn)-350**. Interestingly, upon further heating at 400˚C, the crystal structure expands and a much more open structure is obtained (**MOF(Zn)-2**).

The X-ray intensity data were collected on a Bruker D8 Venture diffractometer (**MOF(Zn), MOF(Zn)-RT, MOF(Zn)-100, MOF(Zn)-350** and **MOF(Zn)-1**) and on a Rigaku Oxford Diffraction Supernova diffractometer (**MOF(Zn)-1** and **MOF(Zn)-2**), using Mo-Kα radiation. The data for **MOF(Zn), MOF(Zn)-RT, MOF(Zn)-100,** and **MOF(Zn)-350** were integrated with SAINT[S6] and corrected for absorption effects with SADABS[S7]. The data for **MOF(Zn)-1** and **MOF(Zn)-2** were processed with CrysAlisPro[S8], and absorption corrections based on multiple-scanned reflections were carried out with SCALE3 ABSPACK in CrysAlisPro. All crystal structures were solved with SHELXT[S9] and refined with SHELXL[S9]. The OLEX2 software was used as a graphical interface [S10]. Anisotropic atomic displacement parameters were introduced for all non-hydrogen atoms. Hydrogen atoms were placed at geometrically calculated positions and refined with the appropriate riding model, with Uiso(H) = 1.2 Ueq(C, O) (1.5 for methyl groups).

Even though crystal data was collected up to 0.77 Angstroms resolution, crystals still diffracted quite weakly at high angle due to their rather low quality (with exception to **MOF(Zn)-RT** and **MOF(Zn)-1**) and data were cut off according to intensity statistics, using restraints and constraints during refinement.

In **MOF(Zn)**, it was not possible to clearly see electron-density peaks in difference maps which would correspond with acceptable locations for the H atoms bonded to O1W. Therefore, the refinement was completed with no allowance for these H atoms in the model. The contributions of these missing atoms (formulae, formula weight, etc.) have been included in the CIF.

In **MOF(Zn)-RT,** a DMF solvent molecule was found disordered over two alternative positions (0.52:0.48 ratio), and was refined with rigid groups, partially equal anisotropic displacement parameters and restraints on geometry and displacement parameters. In this heavy-atom structure it was not possible to clearly see electron-density peaks in difference maps which would correspond with acceptable locations for the H atoms of the disordered DMF molecule. Therefore, the refinement was completed with no allowance for these H atoms in the model. The contributions of these missing atoms (formulae, formula weight, etc.) have been included in the CIF.

During the refinement of **MOF(Zn)-100,** a number of ISOR restraints had to be used to obtain reasonable displacement parameters for all non-hydrogen atoms. Their U_{ij} values were therefore restrained to be approximately spherical. Severely disordered DMF in **MOF(Zn)-100** could not be modelled reasonably, and were therefore removed from the diffraction data (using the OLEX2 Mask tool) but considered for calculation of empirical formula, formula weight, density, linear absorption coefficient and F(000). A solvent mask was calculated and 322.0 electrons were found in a volume of

642.0 $Å^3$ in one void. This is consistent with the presence of 2 DMF molecules per formula unit which account for 320.0 electrons.

A number of ISOR restraints had to be used to obtain reasonable displacement parameters for all non-hydrogen atoms in **MOF(Zn)-350.** Their U_{ij} values were therefore restrained to be approximately spherical. In this heavy-atom structure it was not possible to clearly see electron-density peaks in difference maps which would correspond with acceptable locations for the H atoms bonded to O1W, O2W and O3. Therefore, the refinement was completed with no allowance for these H atoms in the model. The contributions of these missing atoms (formulae, formula weight, etc.) have been included in the CIF.

In **MOF(Zn)-1**, SADI, FLAT, RIGU and EADP commands were used to obtain reasonable geometry and anisotropic displacement parameters for the DMF solvent molecule. This molecule is disordered across a twofold rotation axis; bonds to symmetry equivalents were suppressed using PART -1 command. In this heavy-atom structure it was not possible to clearly see electron-density peaks in difference maps which would correspond with acceptable locations for the H atoms of the disordered DMF molecule. Therefore, the refinement was completed with no allowance for these H atoms in the model. The contributions of these missing atoms (formulae, formula weight, etc.) have been included in the CIF.

Whole molecule disorder of the btca ligand was modelled in **MOF(Zn)-2** via AFIX, DFIX, FLAT, EADP, and RIGU commands. The ratio between the two components was refined freely and converged at 0.48:0.52. A DFIX command was used to restrain the geometry of the μ_2-bridging formato ligand in order to exhibit a O-CH-O moiety between symmetry related Zn2 atoms (symmetry operation: -x, +y, 5/2-z). Figure 1.d. shows a labelled ORTEP plot showing the μ_2-bridging formato ligand linking two symmetry-related half-occupancy Zn2 atoms. Crystal data and refinement details are listed in Table S1.

Table S1. Selected crystallographic data for all compounds.

Compound	**MOF(Zn)-1**					**MOF(Zn)-2**
Activation temperature	**As synthesised**	**24h at RT**	**2h at 100 °C**	**2h at 200 °C**	**2h at 350 °C**	**2h at 400 °C**
Space group	C2/c	C2/c	C2/c	C2/c	C2/c	C2/c
Chemical formula	$C_{20}H_{24}N_8O_9Zn_3$	$C_{20}H_{22}N_8O_8Zn_3$	$C_{20}H_{22}N_8O_8Zn_3$	$C_{17}H_{15}N_7O_7Zn_3$	$C_{14}H_{16}N_6O_{10}Zn_3$	$C_{15}H_7N_6O_7Zn_4$
Formula Mass (g/mol)	716.58	698.56	698.56	625.47	624.44	644.75
***a* (Å)**	17.7182(14)	18.037(2)	18.94(3)	19.2623(14)	19.544(2)	16.643(2)
***b* (Å)**	13.0967(12)	12.5871(13)	10.098(16)	9.9839(6)	9.0665(12)	14.593(2)
***c* (Å)**	11.0610(10)	11.0828(13)	10.957(17)	11.0852(7)	11.0933(13)	10.964(2)
***β* (°)**	94.014(4)	93.046(5)	90.71(4)	90.246(8)	90.176(4)	90.296(16)
***V* (Å^3)**	2560.4(4)	2512.6(5)	2095(6)	2131.8(2)	1965.7(4)	2662.8(7)
Z	4	4	4	4	4	4
T	150 K	120 K	120 K	120 K	120 K	120 K
ρ_{calc} **(g·cm^{-3})**	1.859	1.847	2.215	1.949	2.110	1.608
2*θ* range (°)	2.305 – 22.960	2.658 – 25.197	2.286 – 19.167	3.676 – 25.052	2.476 – 25.051	3.354 – 17.216
Data/Restraints/Parameters	1765/0/195	2238/144/226	848/90/132	1877/27/173	1588/90/150	805/263/156
Nº reflections	15414	7245	7160	16741	5727	6607
Independent reflections [I > 2σ(I)]	1765	2238	848	1877	1588	805
GoF	1.106	1.072	1.664	1.126	1.060	1.165
R Factor [I > 2σ(I)]	R_1 = 0.0402, wR_2 = 0.0828	R_1 = 0.0494, wR_2 = 0.0831	R_1 = 0.1798, wR_2 = 0.4035	R_1 = 0.0296, wR_2 = 0.0666	R_1 = 0.0625, wR_2 = 0.1336	R_1 = 0.1035, wR_2 = 0.2575
R Factor (all data)	R_1 = 0.0587, wR_2 = 0.0891	R_1 = 0.0860, wR_2 = 0.0918	R_1 = 0.2122, wR_2 = 0.4232	R_1 = 0.0349, wR_2 = 0.0689	R_1 = 0.1151, wR_2 = 0.1578	R_1 = 0.1239, wR_2 = 0.2778
CCDC Code	1916085	1916086	1916087	1916083	1916082	1916084

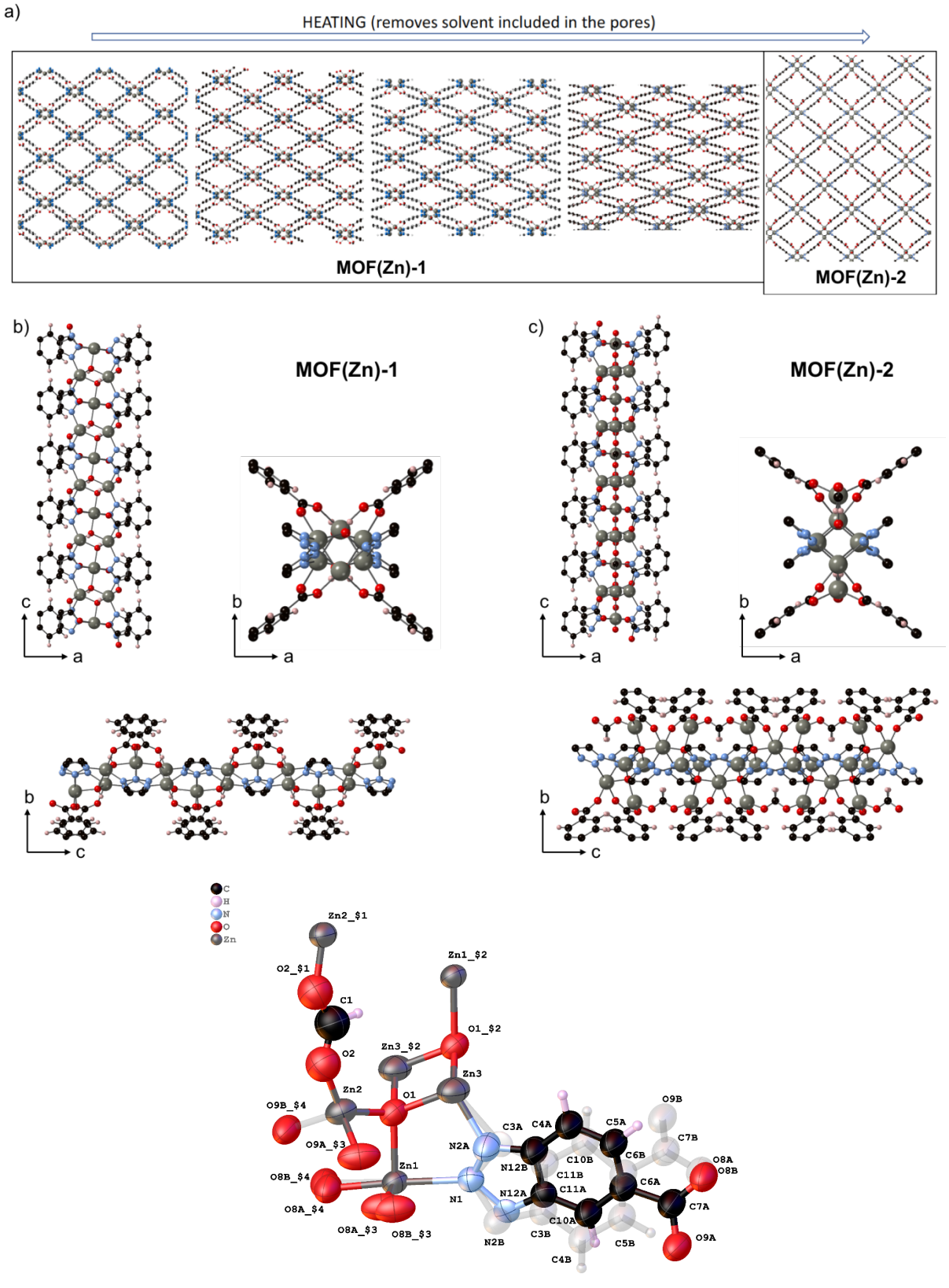

Figure S1. (a) Representation of the different crystal structures obtained during the breathing process upon increasing the temperature. (b) Different views of the structure of MOF(Zn)-1. (c) Different views of the structure of MOF(Zn)-2. (d) A labelled ORTEP plot at 50% probability level of the asymmetric unit of MOF(Zn)-2 showing the μ_2-bridging formato ligand linking two symmetry-related half-occupancy Zn2 atoms and the disordered btca ligand (symmetry operations: \$1: -x, +y, 5/2-z; \$2: -x,-y,2-z; \$3: -1/2-x, 1/2+y, 3/2-z; \$4: 1/2+x, 1/2+y, +z).

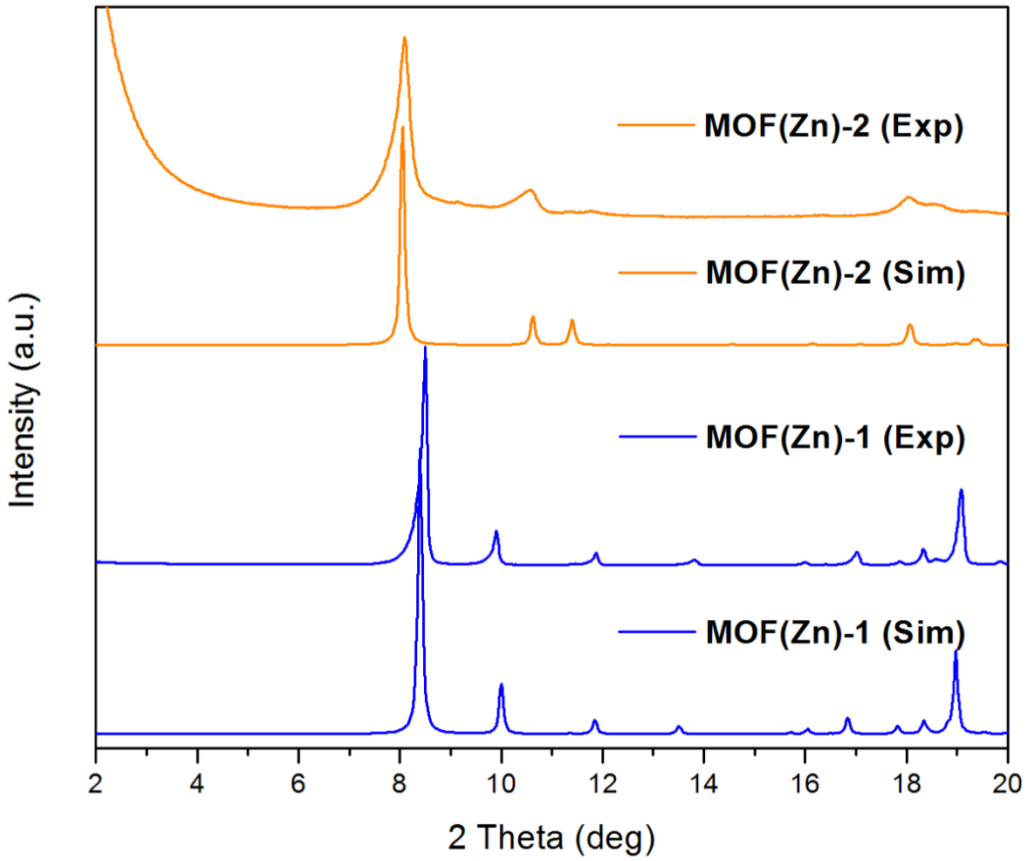

Figure S2. Experimental and simulated PXRD spectra of the MOF activated at 200˚C (**MOF(Zn)-1**) and at 400˚C (**MOF(Zn)-2**).

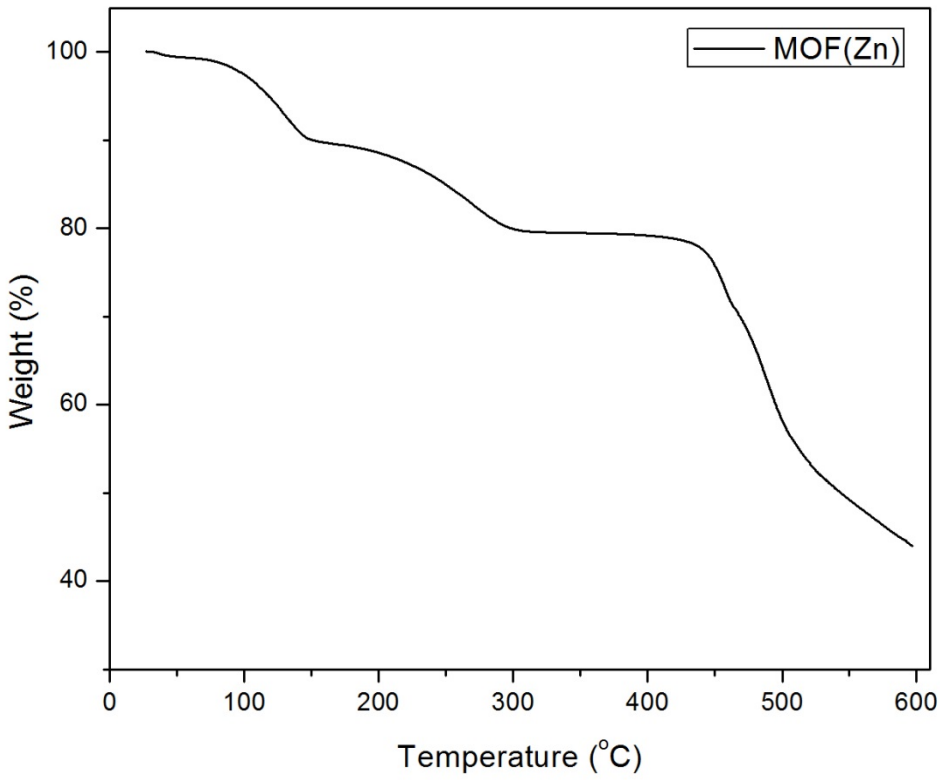

Figure S3. Thermogravimetric analysis (TGA) profile of **MOF(Zn)** at a heating rate of 5ºC/min under a constant stream of N_2.

3. Catalytic tests

Catalyst characterization

High resolution transmission electron microscopy images (HR-TEM) and scanning TEM images in dark field mode (DF-STEM) were recorded on a JEOL JEM2100F instrument operating at 200 kW. An Oxford detector coupled to the STEM instrument was employed to measure the composition of selected MOF areas. The metal particle size distribution and standard deviation were estimated by counting about 300 nanoparticles. The morphology and composition of the MOF samples were further characterized using a scanning electron microscope (SEM, Zeiss instrument, AURIGA Compact) coupled with a EDX detector. Isothermal nitrogen adsorption experiments were carried out using an ASAP 2010 Micromeritics device. X-ray photoelectron (XP) spectra were collected on a SPECS spectrometer with a MCD-9 detector using a monochromatic Al (Kα= 1486.6 eV) X-ray source. Spectra deconvolution was performed with the CASA software using the C 1s peak at 284.4 eV as binding energy reference. Inductively coupled plasma atomic emission spectroscopy (ICP-AES) has been used to confirm the metal content of the catalyst previously digested in concentrated nitric acid. The content of Cu_2O metal loaded was determined by IPC-AES before (0.92% wt Cu) and after (0.89 %wt Cu) use.

Photocatalytic methanation tests

For the photoassisted methanation, a quartz photoreactor equipped with a heating mantle to control the desired temperature during the experiment was utilized. The photocatalyst (15 mg) as powder was placed as a bed inside the reactor, the system was purged and charged with H_2, and then CO_2 was added until a ratio 4 to 1 was achieved. The photoreactor was heated up to 215 °C, once the temperature was stable, the photocatalyst was irradiated under UV-Vis light using a Xe lamp (300 W) as light source. The reaction was monitored by taking periodically gas samples from the reactor that were injected into an Agilent 490 MicroGC equipped with two channels and thermal conductivity detectors. One channel allows analyzing H_2, O_2, N_2 and CO with a MolSieve 5Å column while the other channel shows CO_2, CH_4 and short chain hydrocarbons using a Pore Plot Q column. Gases were quantified calibrating the instrument analyzing of gas mixtures. The limit of detection of the micro-GC of the reaction that is estimated to be below 0.1 $\mu g \cdot cat^{-1} \cdot h^{-1}$.

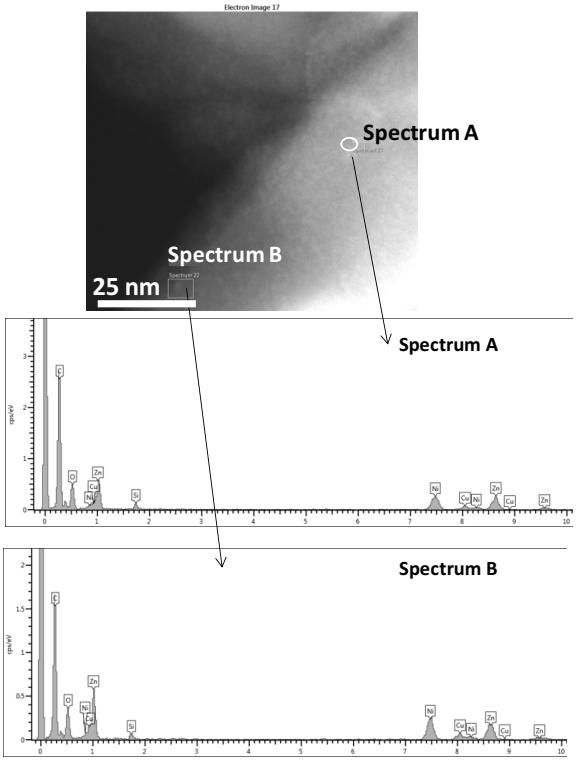

Figure S4. (a) Representative DF-STEM image of Cu_2O@**MOF(Zn)-1**. (b) EDS analysis of two copper nanoparticles (spectrum A and B).

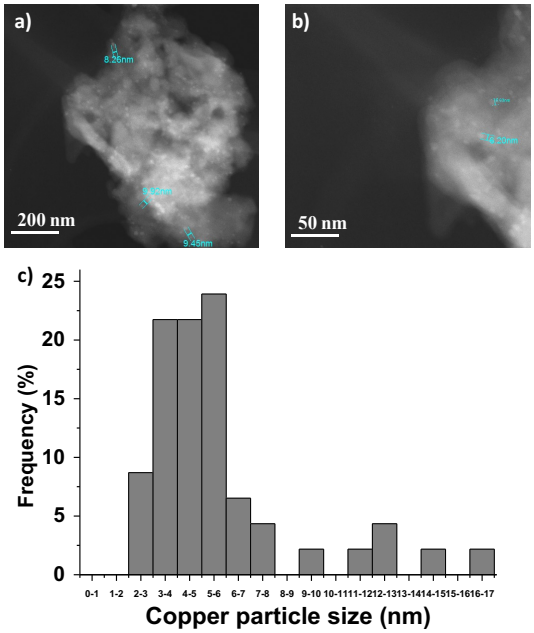

Figure S5. (a,b) DF-STEM images of Cu_2O@**MOF(Zn)-2**. (c) Copper particle size distribution

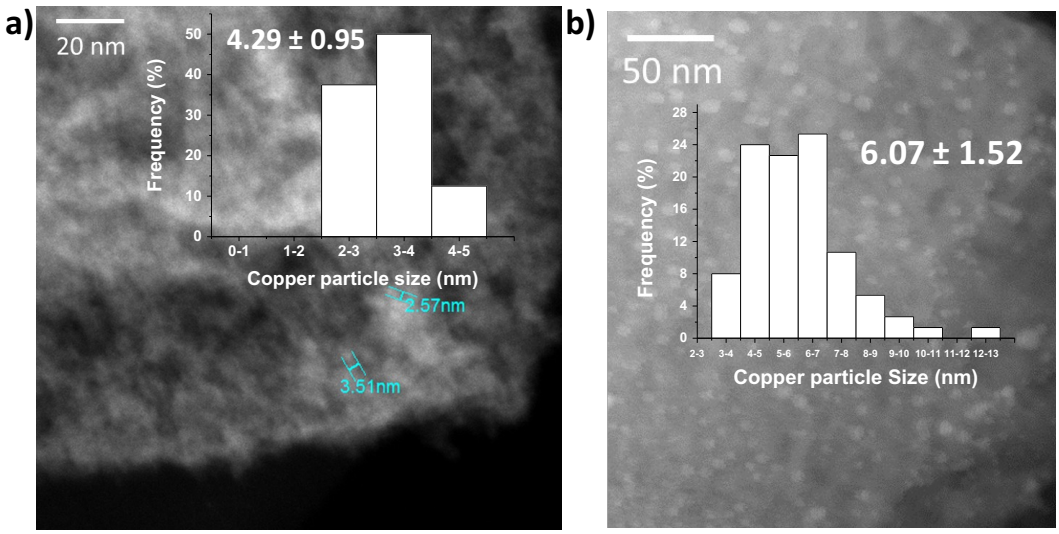

Figure S6. DF-STEM images of (a) Cu_2O@**MIL-125(Ti)-NH_2** and (b,c) Cu_2O@**MOF-74(Zn)**. The insets show the copper particle size distribution, the average copper particle size and standard deviation obtained after counting more than 300 particles.

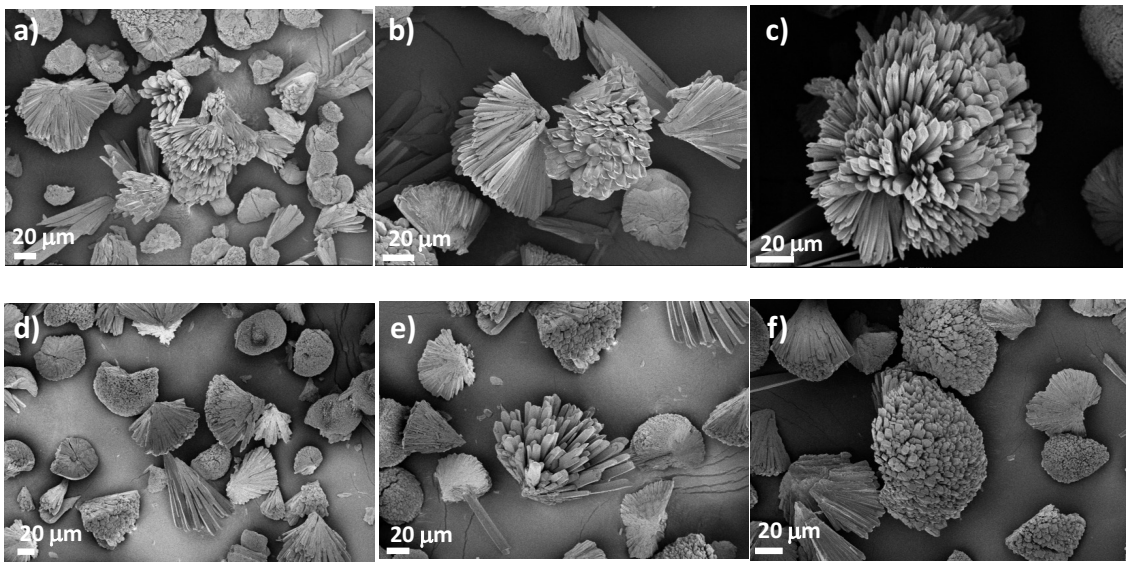

Figure S7. SEM images of (a,b,c) Cu_2O@**MOF(Zn)-1** and (d, e, f) Cu_2O@**MOF(Zn)-2**, revealing the morphology of the crystals.

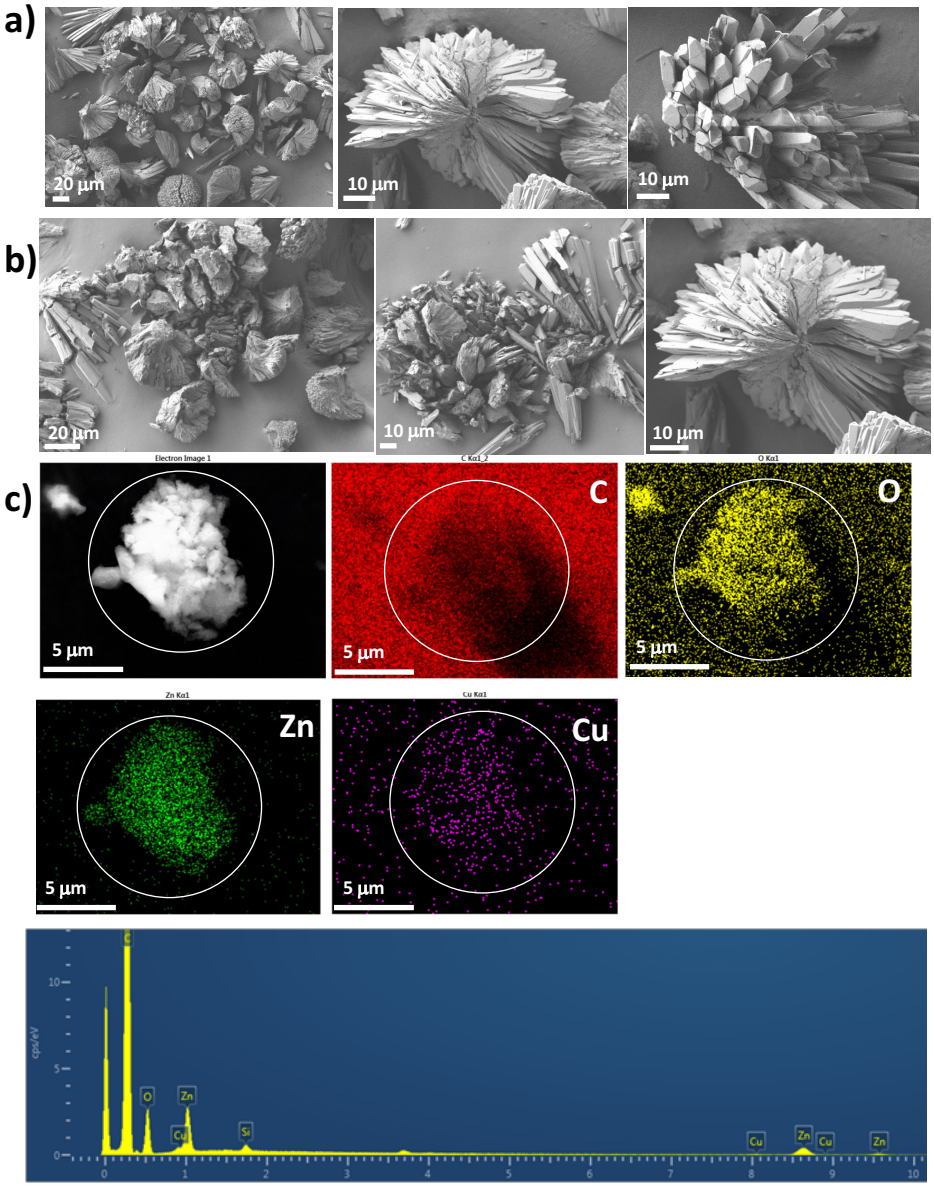

Figure S8. SEM images of (a) Cu_2O@**MOF(Zn)-1** and (b) Cu_2O@**MOF(Zn)-2**. (c) Elemental analysis mapping of a selected area of Cu_2O@**MOF(Zn)-1**.

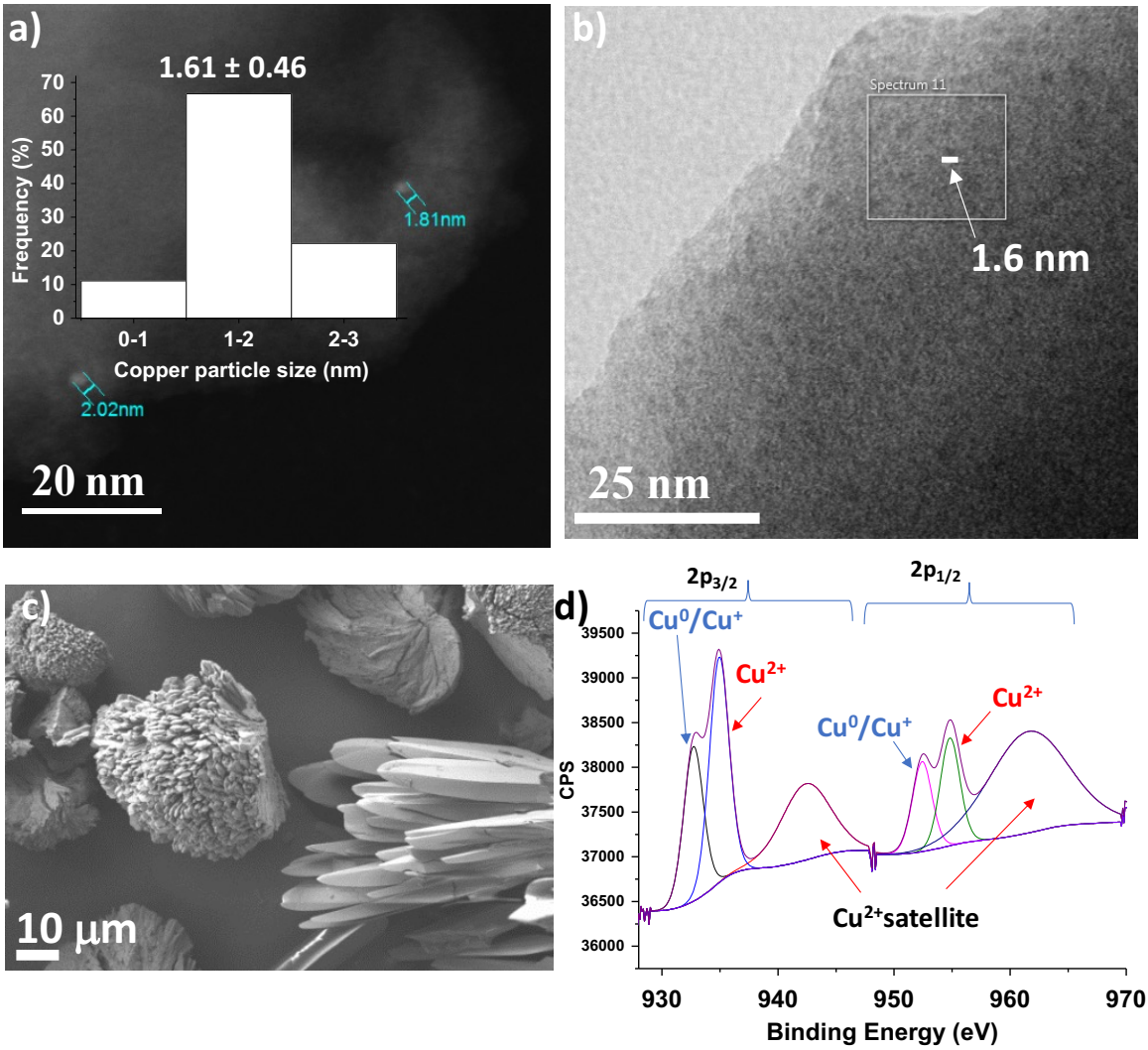

Figure S9. (a) DF-STEM and (b) BF-STEM images of fresh Cu_2O@**MOF(Zn)-1** photocatalyst; the inset corresponds to the copper particle size distribution obtained by counting about 300 particles. (c) SEM image of fresh SEM image and (d) XPS Cu2p spectrum of Cu_2O@**MOF(Zn)-1** showing the best deconvolution to individual components.

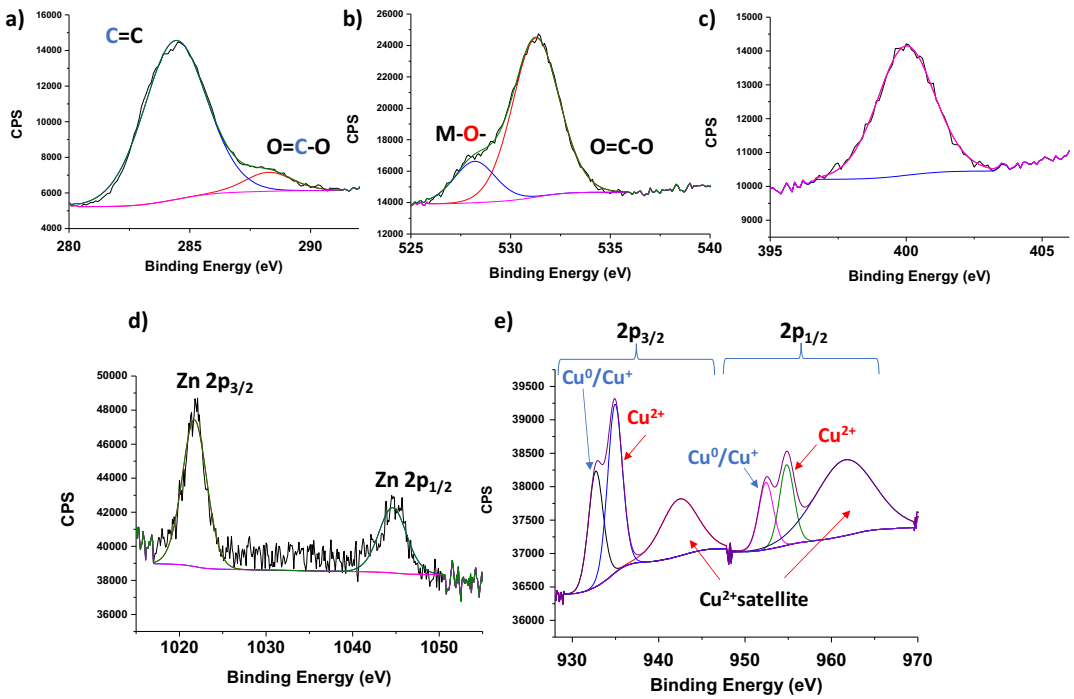

Figure S10. XPS spectra of Cu_2O@**MOF(Zn)-1**. (a) C1s XPS, (b) O1s XPS, (c) N1s XPS, (d) Cu2p XPS, (e) Zn2p XPS.

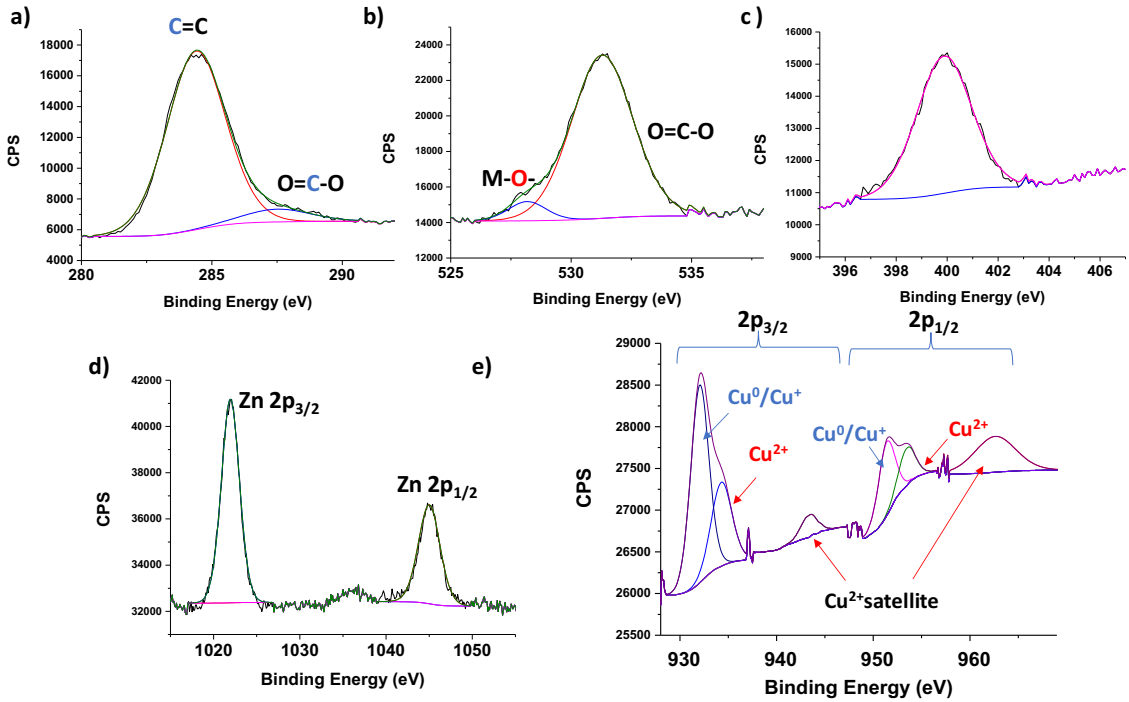

Figure S11. XPS spectra of Cu_2O@**MOF(Zn)-2**. (a) C1s XPS, (b) O1s XPS, (c) N1s XPS, (d) Cu2p XPS, (e) Zn2p XPS.

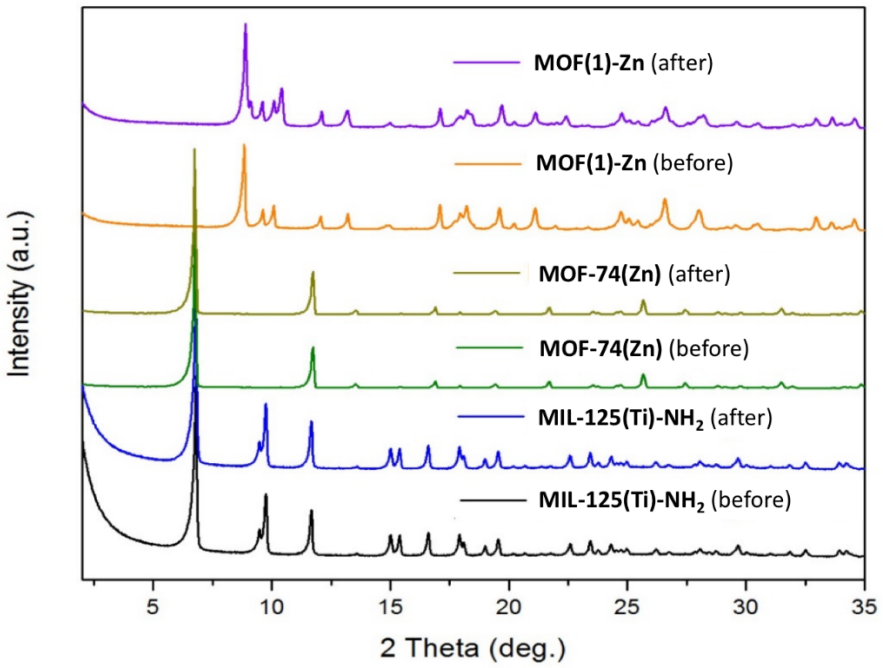

Figure S12. Powder X-ray diffraction patterns of the different copper-supported MOF-based catalysts (**MOF(Zn)-1**, **MOF-74(Zn)** and **MIL-125(Ti)-NH$_2$**) before and after the photocatalytic tests.

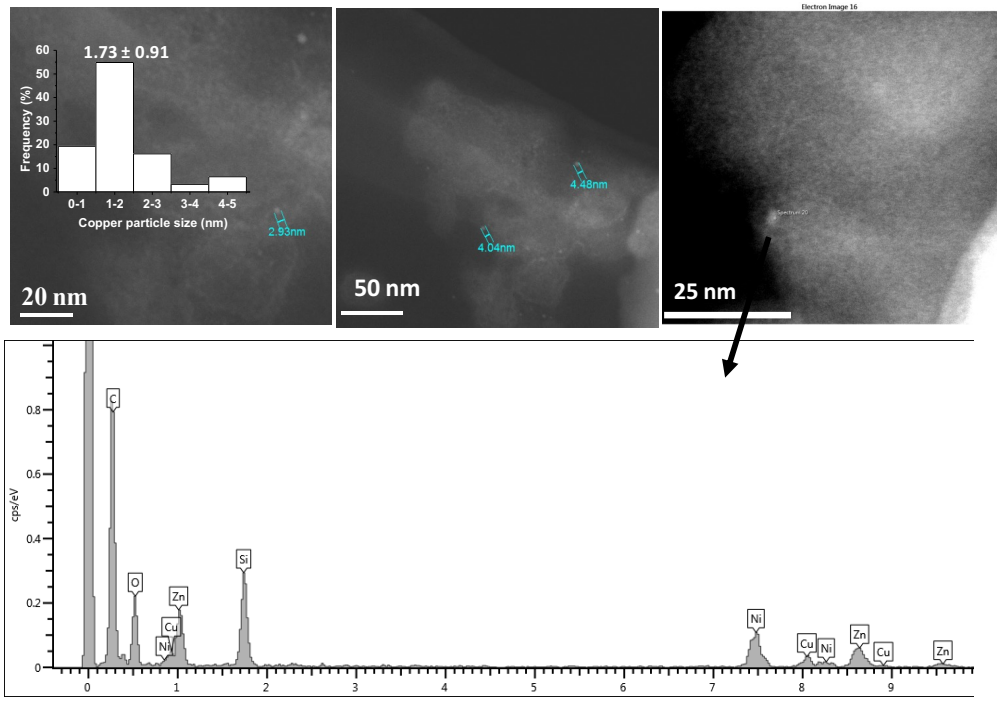

Figure S13. DF-SEM images and EDX spectrum of selected area of Cu_2O@**MOF(Zn)-1** sample after photocatalytic methanation of CO_2.

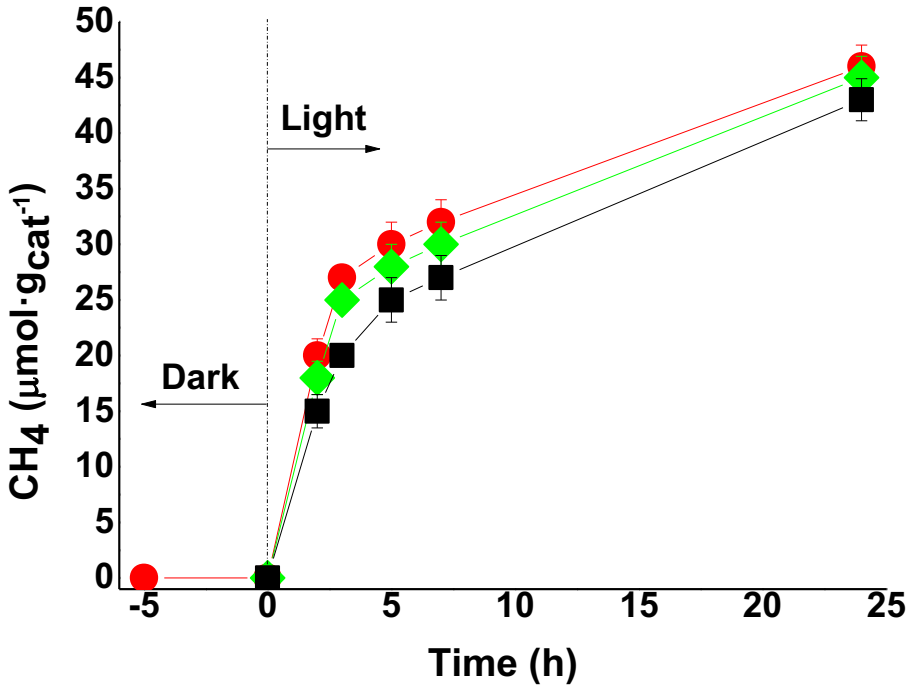

Figure S14. Reusability of Cu_2O@**MOF(Zn)-1** for the CH_4 production at 215 °C upon 2236 W m^{-2} irradiation using a 300 W Xe lamp. PH_2 = 1.05 bar, PCO_2 = 0.25 bar. Legend First use Cu_2O@MOF(Zn)-1 (●), Second use Cu_2O@MOF(Zn)-1 (♦) and third use of Cu_2O@MOF(Zn)-1 (■).

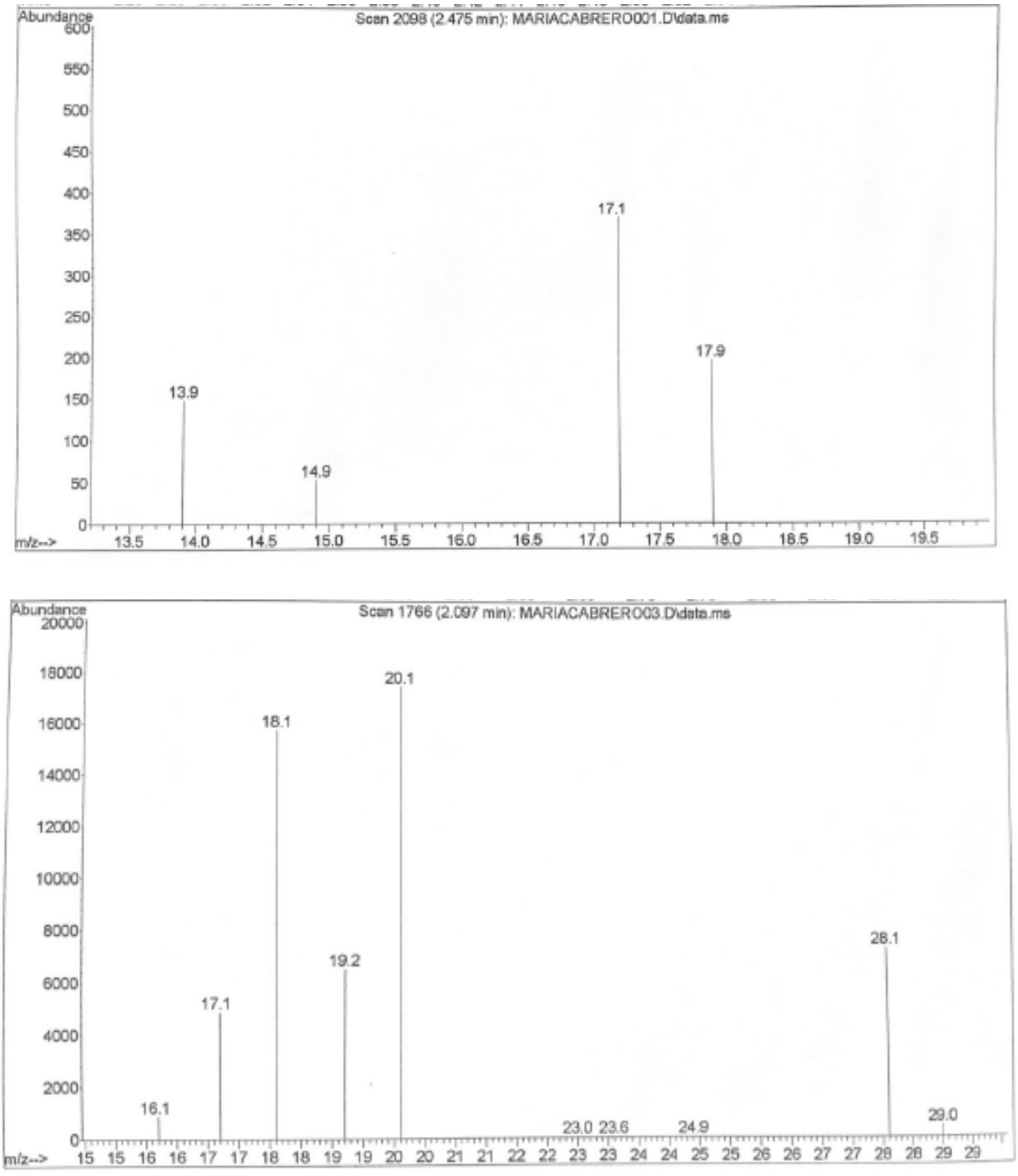

Figure S15. Mass spectra of the reaction products after the photocatalytic reaction using Cu_2O@MOF(Zn)-1 for 22 hours at 215°C using $^{13}C^{18}O_2$.

4. Determination of valence band energies and optical gaps

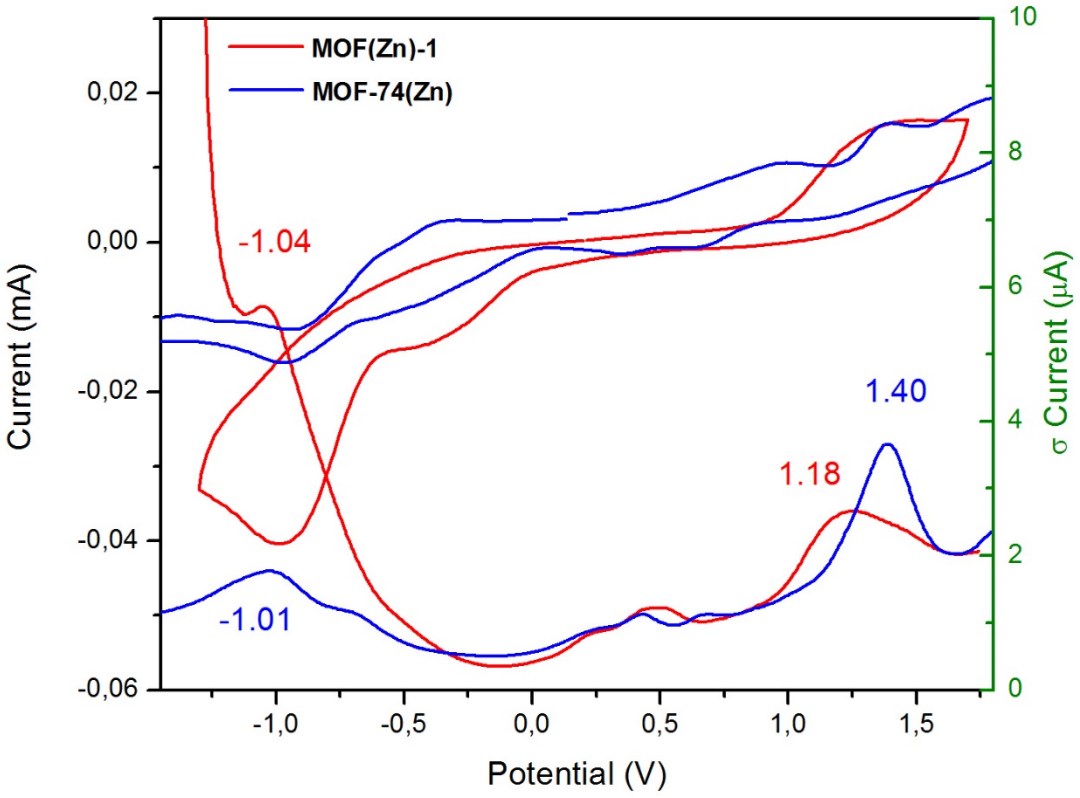

Figure S16. Solid-state Cyclic Voltammetry (CV) and Differential Pulse Voltammetry (DPV) of **MOF(Zn)-1** and **MOF-74(Zn)** using $TBAPF_6$ 0.1 M in CH_3CN as electrolyte and 0.05 V/s scan rate. Platinum wire was used as counter electrode and silver wire as pseudoreference electrode. Ferrocene was added as internal standard. All potentials are reported versus Ag/AgCl.

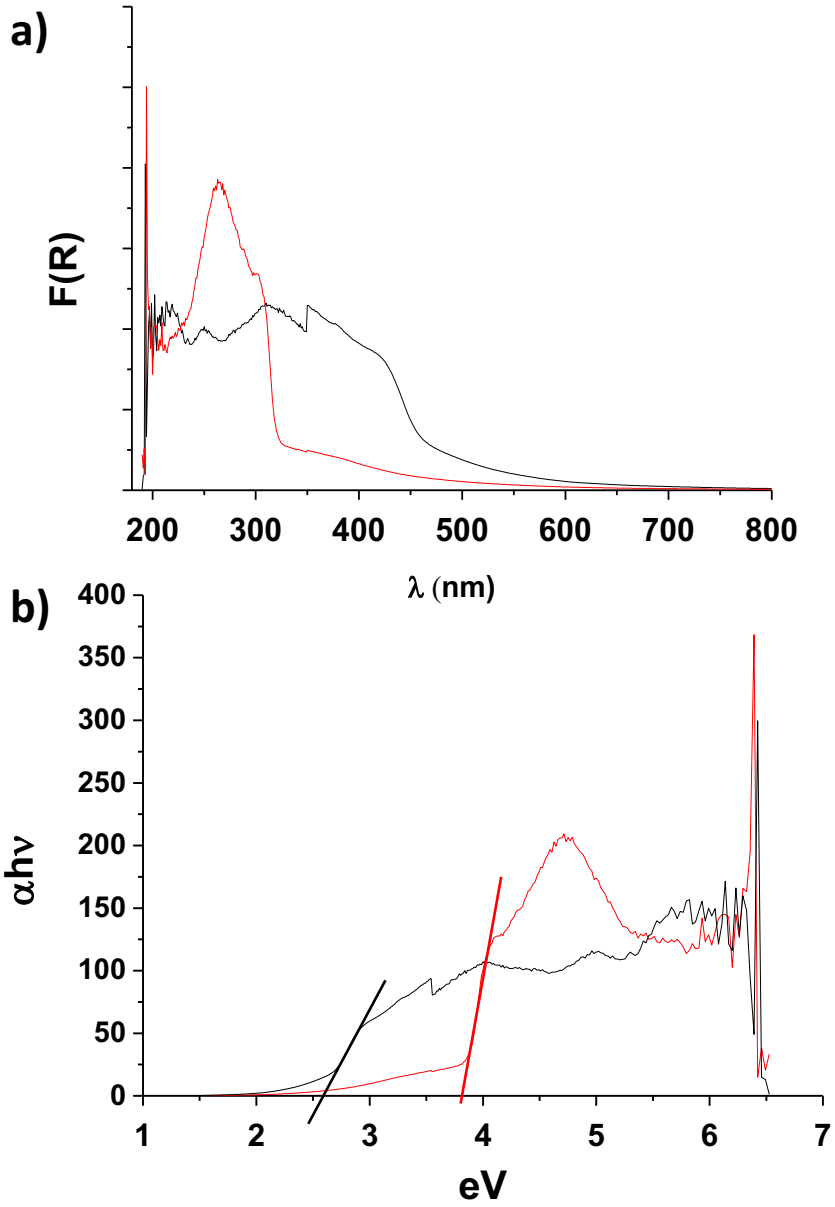

Figure S17. (a) UV-Vis diffuse reflectance and (b) Tauc plot for **MOF(Zn)-1** (red line) and **MOF-74(Zn)** (black line).

5. References

S1. N. Rosi, J. Kim, M. Eddaoudi, B. Chen, M. O'Keeffe and O. M. Yaghi, *J. Am. Chem. Soc.*, 2005, 127, 1504.

S2. M. A. Nasalevich, R. Becker, E. V. Ramos-Fernandez, S. Castellanos, S. L. Veber, M. V. Fedin, F. Kapteijn, J. N. H. Reek, J. I. van der Vlugt and J. Gascón, *Energy Environ. Sci.*, 2015, 8, 364.

S3. S. Remiro-Buenamañana, M. Cabrero-Antonino, M. Martínez-Guanter, M. Álvaro, S. Navalón and H. García, *Appl. Catal. B.-Environ.*, 2019 (accepted).

S4. J. Xiao, Y. Wu, M. Li, B.-Y. Liu, X.-C. Huang and D. Li, *Chem. Eur. J.*, 2013, 19, 1891.

S5. Y. Yue et al. *J. Phys. Chem. C*, 2015, 119, 9442.

S6. SAINT v8.37A, Bruker AXS Inc., Madison, Wisconsin, USA, 2015.

S7. L. Krause, R. Herbst-Irmer, G.M. Sheldrick and D. Stalke. *J. Appl. Cryst.*, 2005, 48, 3.

S8. CrysAlisPro 1.171.38.46. Rigaku Oxford Diffraction, 2015.

S9. G.M. Sheldrick, *Acta Cryst.*, 2015, A71, 3.

S10. O. V. Dolomanov, L. J. Bourhis, R. J. Gildea, J. A. K. Howard and H. Puschmann, *J. Appl. Crystallogr.*, 2009, 42, 339.